High-affinity AKAP7δ–protein kinase A interaction yields novel protein kinase A-anchoring disruptor peptides

Christian HUNDSRUCKER*, Gerd KRAUSE*, Michael BEYERMANN*, Anke PRINZ†, Bastian ZIMMERMANN‡, Oliver DIEKMANN‡, Dorothea LORENZ*, Eduard STEFAN*, Pavel NEDVETSKY*, Margitta DATHE*, Frank CHRISTIAN*, Theresa McSORLEY*, Eberhard KRAUSE*, George McCONNACHIE§, Friedrich W. HERBERG†, John D. SCOTT§, Walter ROSENTHAL*¶ and Enno KLUSSMANN*¶¹

*Leibniz-Institut für Molekulare Pharmakologie, Campus Berlin-Buch, Robert-Rössle-Str. 10, 13125 Berlin, Germany, †Institut für Biochemie, Universität Kassel, Heinrich-Plett-Str. 40, 34109 Kassel, Germany, ‡Biaffin GmbH & Co. KG, Heinrich-Plett-Str. 40, 34132 Kassel, Germany, §Howard Hughes Medical Institute, Vollum Institute, Oregon Health and Science University, Portland, OR 97239, U.S.A., and ¶Institut für Pharmakologie, Charité – Universitätsmedizin Berlin, Campus Benjamin Franklin, Freie Universität Berlin, Thielallee 67–73, 14195 Berlin, Germany

PKA (protein kinase A) is tethered to subcellular compartments by direct interaction of its regulatory subunits (RI or RII) with AKAPs (A kinase-anchoring proteins). AKAPs preferentially bind RII subunits via their RII-binding domains. RII-binding domains form structurally conserved amphipathic helices with un-related sequences. Their binding affinities for RII subunits differ greatly within the AKAP family. Amongst the AKAPs that bind RIIα subunits with high affinity is AKAP7δ [AKAP18δ; K_d (equilibrium dissociation constant) value of 31 nM]. An N-ter-minally truncated AKAP7δ mutant binds RIIα subunits with higher affinity than the full-length protein presumably due to loss of an inhibitory region [Henn, Edemir, Stefan, Wiesner, Lorenz, Theilig, Schmidtt, Vossebein, Tamma, Beyermann et al. (2004) J. Biol. Chem. **279**, 26654–26665]. In the present study, we demonstrate that peptides (25 amino acid residues) derived from the RII-binding domain of AKAP7δ bind RIIα subunits with higher affinity ($K_d = 0.4 \pm 0.3$ nM) than either full-length or N-terminally truncated AKAP7δ, or peptides derived from other RII binding domains. The AKAP7δ-derived peptides and stearate-coupled membrane-permeable mutants effectively disrupt AKAP–RII subunit interactions *in vitro* and in cell-based assays. Thus they are valuable novel tools for studying anchored PKA signalling. Molecular modelling indicated that the high affinity binding of the amphipathic helix, which forms the RII-binding domain of AKAP7δ, with RII subunits involves both the hydrophobic and the hydrophilic faces of the helix. Alanine scanning (25 amino acid peptides, SPOT technology, combined with RII overlay assays) of the RII binding domain revealed that hydrophobic amino acid residues form the backbone of the interaction and that hydrogen bond- and salt-bridge-forming amino acid residues increase the affinity of the interaction.

Key words: A kinase-anchoring protein 7 (AKAP7), aquaporin-2 (AQP2), molecular modelling, peptide disruptor, protein kinase A (PKA) anchor, RII-binding domain.

INTRODUCTION

A plethora of stimuli including hormones and neurotransmitters induce the generation of the second messenger cAMP and thereby mediate activation of PKA (protein kinase A) in the same cell, often at the same time. It is now appreciated that different stimuli induce the activation of PKA at specific sites within a cell [1]. Local activation of PKA allows for the phosphorylation of parti-cular substrates in close proximity and is facilitated by the tethering of PKA to cellular compartments by AKAPs (A kinase-anchoring proteins; [2–4]). The compartmentalization of PKA by AKAPs contributes to the specificity of a cAMP-dependent cellular response. However, localization of PKA by itself may not be sufficient to compartmentalize a cAMP-/PKA-dependent pathway. As cAMP readily diffuses throughout the cell, discrete cAMP signalling compartments are only conceivable if this dif-fusion is restricted. This is achieved by the action of PDEs (phosphodiesterases). They establish gradients of cAMP by local hydrolysis of the second messenger. For example, PDE3 and PDE4 localize to distinct compartments in cardiac myocytes. PDE4, rather than PDE3, appears to modulate the amplitude and

duration of the cAMP response to β-adrenergic receptor activation [5]. A few PDEs interact with AKAPs and thus establish local control of the cAMP concentration at the site of PKA action [6].

Several AKAPs bind not only PKA and PDEs but also other signalling molecules. They form multiprotein complexes that propagate and integrate a broad range of cellular events [2]. For example, AKAP13 (AKAP-Lbc or AKAP-Ht31) binds three protein kinases: PKA, PKC (protein kinase C) and protein kinase D, and functions as a guanine nucleotide exchange factor for the small GTPase, Rho A [7–12].

The inactive PKA holoenzyme consists of two C (catalytic) and dimeric R (regulatory) subunits, type RI (RIα or RIβ) or type RII (RIIα or RIIβ). Binding of cAMP to the R subunits causes a con-formational change, resulting in the release and, thereby, ac-tivation of the C subunits [13,14]. AKAPs preferentially interact with RII subunits, although some AKAPs also bind RI subunits [15].

The PKA-anchoring domains, also termed RII-binding do-mains, of AKAPs comprise 14–18 amino acid residues and are structurally conserved within the AKAP family. They form amphipathic helices which slot into a complementary binding

pocket formed by the docking and dimerization domains of the R subunits [16–18]. Sequence homology of RII-binding domains is hardly detectable [19]. The binding affinities for RII subunits differ greatly within the AKAP family. For example, the members of the ERM (ezrin, radixin, moesin) family bind RII subunits with a micromolar affinity [20], whereas AKAP5 (AKAP79), AKAP8 (AKAP95) and AKAP13 bind RII subunits with K_d (equilibrium dissociation constant) values of 1.3–50 nM [21–23] and are considered high affinity AKAPs. AKAP7δ (AKAP18δ; [24]) is also a high affinity AKAP. The K_d values for the binding of AKAP7δ to RIIα and RIIβ subunits are 31 and 20 nM respectively [25]. A truncated AKAP7δ mutant (full-length protein: 353 amino acid residues) consisting of amino acid residues 124–353 binds both RIIα and RIIβ subunits of PKA with higher affinity than the full-length protein (9 and 4 nM respectively). Thus an N-terminal region interferes with RII subunit binding [25]. In the present study, we describe 25 amino acid peptides derived from the AKAP7δ RII-binding domain that bind RII subunits with higher affinity ($K_d = 0.4$ nM) than the full-length protein, the N-terminally truncated mutant (as described above), and peptides derived from other AKAPs. The AKAP7δ-derived peptides disrupt PKA-anchoring *in vitro* and *in vivo* and are thus valuable tools to study anchored PKA signalling.

The interaction of RII-binding domains with RII subunit dimers is considered to be mediated by hydrophobic contacts [18,19,26]. However, the number and distribution of hydrophobic amino acid residues in RII-binding domains is similar in all AKAPs. Hydrophobicity of RII-binding domains, therefore, is most probably not the sole determinant of AKAP–RII interactions. In order to gain further insight into the molecular determinants of the interaction between AKAPs and RII subunits we analysed the interaction of the high-affinity AKAP7δ with RIIα subunits. Our analysis revealed that in addition to hydrophobic interactions, hydrogen bonds and salt-bridges on the hydrophilic face of the amphipathic helix forming the RII-binding domain contribute to binding.

EXPERIMENTAL

Peptides, peptide arrays and RII overlays

Peptides (for sequences see Table 1 and Supplementary Table 1 at http://www.BiochemJ.org/bj/396/bj3960297add.htm) derived from the RII-binding domains of AKAPs were synthesized as described [27]. AKAP7δ-derived peptides were named after the substitution compared with the corresponding position in the full-length AKAP7δ protein e.g. peptide AKAP7δ-L304T-pep comprises amino acid residues 296–320 of AKAP7δ with a leucine to threonine substitution at position 304 in AKAP7δ. Peptides with double or multiple substitutions were named accordingly. AKAP7δ-wt (wild-type)-pep comprises the wt sequence of the AKAP7δ RII-binding domain. For SPR (surface plasmon resonance) and CD measurements (as described below) biotin was attached N-terminally. Peptides were rendered membrane-permeable by N-terminal elongation with stearic acid. The identity of peptides was demonstrated using MS, and their purities were > 90 % as determined by HPLC analysis (220 nm).

Peptide substitution arrays were generated by automatic SPOT-synthesis on Whatman 50 cellulose membranes by using Fmoc (fluoren-9-ylmethoxycarbonyl) chemistry and the AutoSpot-Robot ASS 222 (Intavis Bioanalytical Instruments AG, Köln, Germany) as described in [28,29]. Control spots (approx. 50 nmol of peptide per spot) were excised from the cellulose membrane and analysed by MALDI–TOF (matrix-assisted laser-desorption ionization–time-of-flight)-MS.

Table 1   Peptide sequences

AKAP$_{IS}$ represents a synthetic RII subunit-binding peptide [21]. All other peptides are derived from the RII-binding domains of the indicated AKAPs.

Peptide	Sequence
AKAP$_{IS}$	QIEYLAKQIVDNAIQQA
AKAP$_{IS-P}$	QIEYLAKQIPDNAIQQA
Ht31	KGADLIEEAASRIVDAVIEQVKAAG
Ht31-P	KGADLIEEAASRIPDAPIEQVKAAG
AKAP7δ-wt-pep	PEDAELVRLSKRLVENAVLKAVQQY
AKAP7δ-L304T-pep	PEDAELVRTSKRLVENAVLKAVQQY
AKAP7δ-L308D-pep	PEDAELVRLSKRDVENAVLKAVQQY
AKAP7δ-P-pep	PEDAELVRLSKRLPENAVLKAVQQY
AKAP7δ-PP-pep	PEDAELVRLSKRLPENAPLKAVQQY
AKAP7δ-L314E-pep	PEDAELVRLSKRLVENAVEKAVQQY
AKAP1-pep	EEGLDRNEEIKRAAFQIISQVISEA
AKAP2-pep	LVDDPLEYQAGLLVQNAIQQAIAEQ
AKAP5-pep	QYETLLIETASSLVKNAIQLSIEQL
AKAP9-pep	LEKQYQEQLEEEVAKVIVSMSIAFA
AKAP10-pep	NTDEAQEELAWKIAKMIVSDIMQQA
AKAP11-pep	VNLDKKAVLAEKIVAEAIEKAEREL
AKAP12-pep	NGILELETKSSKLVQNIIQTAVDQF
AKAP14-pep	TQDKNYEDELTQVALALVEDVINYA
Rab32-pep	ETSAKDNINIEEAARFLVEKILVNH

RII-binding of SPOT-synthesized peptides was detected by RII overlays using ^{32}P-labelled recombinant human or mouse RIIα, rat RIIβ, or a combination of bovine RIIα and RIIβ subunits [specific activity of RII subunits = $(1.4 \pm 0.3) \times 10^8$ c.p.m./μg of protein per ml of hybridization solution] [30,31]. Bovine RII subunits were purchased from Sigma–Aldrich (Deisenhofen, Germany), other RII subunits were prepared as described in [23].

SPR measurements

SPR measurements were carried out using a Biacore 2000 instrument (Biacore AB, Uppsala, Sweden) [23]. In brief, CM-5 chips (research grade, Biacore AB), coated with streptavidin [200 RU (resonance units); Sigma–Aldrich Chemie GmbH, Steinheim, Germany], were used to capture N-terminally biotinylated AKAP7δ-derived peptides (Table 1). All subsequent interaction studies were performed in running buffer [20 mM Mops, 150 mM NaCl (pH 7.0) and 0.005 % surfactant P20] at 25 °C. Non-specific binding was subtracted on the basis of blank surfaces with streptavidin-coated flow cells saturated with either biotin or an appropriate negative control peptide. Regulatory RIIα (human; cAMP-free) was injected for 180 s with a flow rate of 50 μl/min using a series of dilutions (0.5 nM to 1 μM). After each injection the dissociation phase was monitored for 600 s. Kinetic constants from the raw data were calculated by non-linear regression or equilibrium binding analysis using the Biaevaluation software version 4 (Biacore AB). K_d values were calculated from the respective rate constants on the basis of a Langmuir 1:1 binding model.

CD measurements

CD measurements of N-terminally biotinylated peptides at a concentration of 50 μM were performed in a mixture of phosphate buffer (10 mM, pH 7.4)/TFE (trifluoroethanol) (1:1, v/v) and, as a control in phosphate buffer (10 mM, pH 7.4) in the presence of 15 mM SDS in a 2 mm cell. Spectra were recorded between 195 and 260 nm on a J-720 spectrometer (Jasco, Japan). The α-helicity (α) of the peptides was determined from the $[\theta]_{m.r.w.}$ (mean residue ellipticity) at 222 nm according to the equation α (%) $= -\{([\theta]_{m.r.w.} + 2340) \times 100\}/30\,300$ [32].

Molecular modelling and structure prediction

For the RII-binding domains of AKAP5 and AKAP13, α-helical structures have been determined by NMR [18,26]. Therefore AKAP7δ-derived peptides were docked into the dimerization/docking domain of RIIα subunits (NMR structures of RIIα dimers are from PDB entries 1R2A and 1L6E that were used as templates) as α-helical structures by utilizing the tools 'surfaces with electrostatic potentials' and 'FlexX' from the SYBYL 6.91 molecular modelling package (TRIPOS Inc., St. Louis, MO, U.S.A.). The peptide and dimerization domain complex with fitting shape, complementary electrostatic potentials on the surfaces and the highest average docking score among the C-Scores (ChemScore, D_Score_G_Score_PMF Score) was selected as the best complex. The model of the complex was placed in a water box and minimized with the AMBER 7.0 force field [33] using the conjugated gradient method by 3000 iterations up to the termination gradient of 0.1 kcal/(mol*A) (1 kcal $\approx$ 4.184 kJ). The geometrical quality of the model was validated with PROCHECK [34]. Secondary structures of the indicated peptides were predicted using the PSIPRED program (http://bioinf.cs.ucl.ac.uk/psipred/).

ELISA-based assay to measure GST (glutathione S-transferase)–AKAP7δ–RIIα interaction

Multiwell plates (Corning B.V. Life Sciences, Schiphol-Rijk, The Netherlands) were coated with RIIα (15 ng/well) by incubation in PBS containing protease inhibitors (1 h, 22 °C). Free binding sites were blocked by incubation with blocking buffer (PBS containing 0.3 % dried skimmed milk/0.05 % Tween-20) for 1 h at 22 °C. After washing three times with wash buffer (PBS/0.05 % Tween-20), GST–AKAP7δ ([25];15 ng/well) was added in the absence or presence of peptides (concentrations are indicated in Figure 2A). As a control, the peptide solvent, DMSO, was added without peptide in appropriate concentrations. DMSO did not affect the binding of GST–AKAP7δ to RIIα subunits. After incubation for 1 h at 22 °C and washing with wash buffer, rabbit anti-AKAP7δ (A18δ3) and peroxidase-conjugated anti-rabbit antibodies were added for 1 h at 22 °C. The wells were rinsed with wash buffer, LumiLight Western blotting substrate solution (Roche Diagnostics, Mannheim, Germany) was added, and enzyme activity was assessed in a Luminescence intensity reader (GeniosPro, Tecan, Durham, NC, U.S.A.) with 10 ms integration time/well. Curves were fitted based on a one-site-competition binding model and IC_{50} values were calculated using Prism 4.0 (GraphPad Software, San Diego, CA, U.S.A.).

Immuno-isolation of AQP2 (aquaporin-2)-bearing vesicles and PKA activity measurements

AQP2-bearing vesicles were immuno-isolated from rat renal inner-medullary tissue utilizing Eupergit C1Z methylacrylate microbeads (Roehm Pharma, Darmstadt, Germany) coated with anti-AQP2 antibodies (AQP2 antibody beads). Non-specific binding sites on the beads were blocked with glycine. As a control, cellular fractions were prepared with beads coated with glycine alone [25]. Both fractions were resuspended in PBS, and PKA activity was measured using a commercially available assay system based on PKA phosphorylation of the substrate peptide Kemptide (Upstate Cell Signaling Solutions/Biomol, Hamburg, Germany).

Electrophysiology

Cardiac myocytes were obtained from 3–5-day-old neonatal rats and cultured as described [35]. The whole-cell L-type I_{Ca} (Ca^{2+} current) was recorded at room temperature from spontaneously contracting cells 3–5 days after seeding [36] (EPC-9 patch clamp amplifier, Pulse software, HEKA Elektronik, Lambrecht, Germany). The extracellular solution contained 140 mM TEA chloride, 10 mM Hepes, 1 mM $MgCl_2$, 2 mM $CaCl_2$, 12 mM glucose and 0.1 mM EGTA (pH 7.4 adjusted with CsOH; 300 mOsm/kg). The intracellular solution contained 80 mM CsCl, 15 mM TEA chloride, 20 mM citrate, 10 mM Hepes, 2 mM $CaCl_2$, 3 mM $MgCl_2$, 5 mM EGTA, 10 mM MgATP, 0.3 mM Na-GTP, 0.2 mM free Mg^{2+} and 45 nM free Ca^{2+} (pH 7.4, adjusted with CsOH; 285 mOsm/kg; Ca^{2+} and Mg^{2+} concentrations were calculated with Win-MAXC (http://www.stanford.edu/~cpatton/winmaxc2.html). Fire-polished recording pipettes (borosilicate glass) were filled with intracellular solution and had a resistance of 2–3 MΩ. To evoke I_{Ca}, cells were depolarized repetitively (20 s intervals) from a holding potential of -70 mV to -35 mV with a 400 ms ramp and then depolarized to a test potential of 0 mV for 100 ms. All membrane potentials were corrected for liquid junction potential (11 mV). The currents were filtered at 2.9 kHz and sampled at 2 kHz. If necessary currents were leak-subtracted by the P/4 method. I_{Ca} was measured as the difference between the peak inward current and the current at the end of the test pulse [37]. Series resistance (4–10 MΩ) and total C_m (membrane capacitance) were compensated and continuously recorded. For a comparison of different cells' current densities, I_{Ca}/C_m was calculated. Peptides (30 μM, dissolved in intracellular solution, DMSO content $\leqslant 0.16$ %) were introduced into the cells via the patch pipette. The influence of peptides on the isoproterenol stimulation of L-type Ca^{2+} channels was measured for 11 min (for peptides used at 30 μM) or 22 min (for peptides used at 1 μM) after patch rupture. Isoproterenol (1 μM) was applied through an application pipette (QMM, Ala Scientific Instruments) positioned near the cell. For statistical analysis (one-way ANOVA) isoproterenol-evoked I_{Ca}/IC_m was expressed as a fraction of unstimulated I_{Ca}/IC_m.

BRET (bioluminescent resonance energy transfer) measurements

Generation of the BRET sensor and BRET measurements were carried out as recently described [38]. In brief, the human PKA Cα subunit-encoding sequence was amplified by using sense and anti-sense primers harbouring HindIII and BamHI sites respectively, and subcloned into the corresponding restriction enzyme sites of the vector pGFP (green fluorescent protein)-C3 (PerkinElmer Rodgau, Germany). The human PKA RIIα subunit-encoding sequence was amplified with primers allowing for cloning with BamHI and KpnI restriction enzymes into the vector pRluc-N2 (PerkinElmer). COS-7 cells, maintained in DMEM (Dulbeco's modified Eagles's medium) plus 10 % foetal calf serum, were seeded in a 96-well microplate (Optiplate, PerkinElmer; 2×10^4 cells/well). Co-transfections were carried out 1 day later using 4 μl of PolyFect (Qiagen, Hilden, Germany) and a total of 0.5 μg of plasmid DNA/well. After 2 days, cells were serum-starved for 4 h, and subsequently rinsed with D-PBS (Dulbecco's-PBS), (Invitrogen, Karlsruhe, Germany). 8-Br-cAMP-AM (8-bromo-cAMP-acetoxymethylester; 50 μM; [39]) or the membrane-permeable stearate-coupled peptides S–AKAP7δ-L314E-pep, S–Akap7δ-PP-pep, S–Ht31 or S–Ht31-P (100 μM each) were added to the wells for 30 min. The cells were incubated with 100 μM isoproterenol or, as a control, with D-PBS (10 min). Liquid was removed from the wells, and BRET measurements were started by adding 5 μM DeepBlueC™ (PerkinElmer). The emission of light was detected using a Fusion™ multilabel reader (PerkinElmer) consecutively for each well, using filters at 410 nm wavelength (± 80 nm band pass)
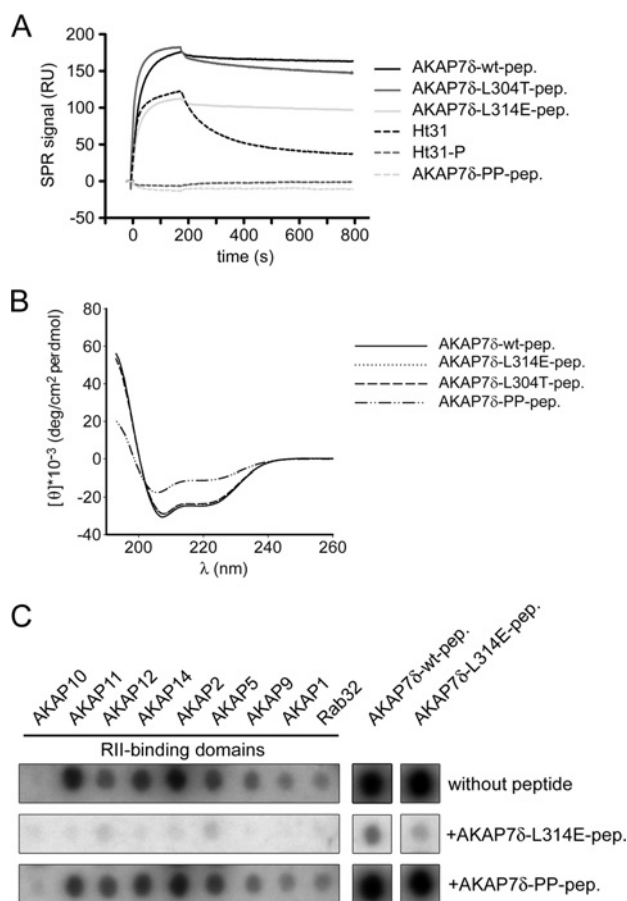
Figure 1 AKAP7δ-derived peptides bind RII subunits of PKA with higher affinity than peptides derived from RII-binding domains of other AKAPs

The sequences of the peptides are given in Table 1. (**A**) SPR measurements to determine the association and dissociation rate constants for the binding of the indicated peptides to human RIIα subunits (500 nM). The plots show representative experiments for each interaction ($n=3$ independent experiments). RU, resonance units. (**B**) CD spectra to determine the α-helicity of the indicated peptides. The helicities (α) of the indicated peptides [each 50 μM in buffer/TFE (1:1, v/v)] were calculated from the mean residue ellipticity [θ] at 222 nm (as described in the Experimental section). The Figure shows representative spectra from at least three independent measurements of each peptide. (**C**) Peptides derived from the RII-binding domains of the indicated AKAPs, and peptide AKAP7δ-L314E-pep derived from the RII-binding domain of AKAP7δ were SPOT-synthesized and probed with ^{32}P-labelled RIIα subunits alone (upper panel), in the presence of the PKA-anchoring disruptor peptide AKAP7δ-L314E-pep (10 μM; middle panel) or the inactive control peptide AKAP7δ-PP-pep (10 μM; lower panel). Signals were detected by autoradiography. A representative experiment is shown ($n=3$ independent experiments).

for the donor (Rluc) and at 515 nm ($\pm$ 30 nm band pass) for the acceptor fluorophore, GFP. Control transfections with empty pRluc and pGFP vectors were performed in each experiment. Background values obtained using untransfected cells were subtracted from each measurement. BRET ratios were calculated as follows using Prism 4.0: (emission $_{515nm}$ − background $_{515nm}$)/ (emission $_{410nm}$ − background $_{410nm}$).

RESULTS

Peptides derived from the RII-binding domain of AKAP7δ bind RII subunits of PKA with subnanomolar affinity

Truncated AKAP7δ (amino acid residues 124–353) binds RII subunits with higher affinity than the full-length protein [25].

Table 2 Equilibrium dissociation constants of the interaction of AKAP7δ-derived peptides (25-mers; for sequences see Table 1) with human RIIα subunits

K_d values are the means $\pm$ S.E.M. n.b., no binding.

Peptide	RIIα K_d (nM)
AKAP7δ-wt-pep	0.4 $\pm$ 0.3
AKAP7δ -L304T-pep	1.2 $\pm$ 1.1
AKAP7δ-L314E-pep	0.7 $\pm$ 0.5
AKAP7δ-L308D-pep	n.b.
AKAP7δ-PP-pep	n.b.

SPR measurements (Figure 1A, Table 2) showed that peptides (25 amino acid residues) representing the RII-binding domain of AKAP7δ (peptide AKAP7δ-wt-pep) bound human RIIα subunits with a K_d value of 0.4 $\pm$ 0.3 nM. That was at least one order of magnitude lower than corresponding K_d values obtained using full-length AKAP7δ, truncated AKAP7δ (amino acid residues 124–353) or with the previously characterized RII-binding peptide Ht31 [23]. Peptide Ht31 represents the RII-binding domain of AKAP13. Single amino acid substitutions introducing polar or charged amino acid residues (peptides AKAP7δ-L314E-pep and AKAP7δ-L304T-pep) did not change the affinity of the AKAP7δ-derived peptide significantly (Figure 1A, Table 2). By contrast, introduction of two α-helix-disrupting prolines (peptides Ht31-P and AKAP7δ-PP-pep) abolished RII-binding (Figure 1A, Table 2). The introduction of a negative charge by replacing leucine with aspartate at position 308 (L308D) also abolished binding to RIIα subunits (Table 2).

TFE-induced helicity of peptides is considered to be indicative of their capability to form α helices [40]. We took the different CD profiles (Figure 1B) as an expression of the different helical propensities of the AKAP7δ-derived peptides. The α-helical (amphipathic helix) content of the peptides AKAP7δ-wt-pep (72 %), AKAP7δ-L314E-pep (70 %) and AKAP7δ-L304T-pep (69 %) were hardly distinguishable from each other and were similar to those of the peptide Ht31 and the RII-binding domain of AKAP5 [18,26]. As expected, the α-helical content of the proline-containing AKAP7δ-PP-pep was strongly decreased (29 %). A comparable helix pattern was found in the presence of membrane-mimicking SDS micelles where the RIIα subunit-binding peptides revealed 54 % helicity, whereas the helical content of peptide AKAP7δ-PP-pep was only 14 % (results not shown).

In order to compare the ability of RIIα subunit binding of AKAP7δ-derived peptides with peptides derived from the RII-binding domains of other AKAPs, we utilized a combination of peptide SPOT technology and RII overlay. Peptides (25 amino acid residues) encompassing the RII-binding domains of the human AKAPs, AKAP1 (AKAP149), 2 (AKAP-KL), 5 (AKAP79), 9 (AKAP450), 10 (D-AKAP2), 11 (AKAP220), 12 (gravin), 14 (AKAP28), Rab32 (Figure 1C), and AKAP13, AKAP$_{IS}$ (AKAP *in silico*) and AKAP7δ-derived peptides (Figures 1C and 2B) were SPOT-synthesized and overlaid with ^{32}P-labelled RIIα subunits. AKAP$_{IS}$ [21] is an RII-binding peptide that has recently been identified by an bioinformatics approach. Figures 1(C) and 2(B) show that AKAP7δ-derived peptides bind RIIα subunits with the highest apparent affinity of all peptides tested. This is supported by the observation that pre-incubation of ^{32}P-labelled RII subunits with peptide AKAP7δ-L314E-pep (10 μM) prevented binding to all peptides except to AKAP7δ-derived ones (Figure 1C and 2B). Pre-incubation of RIIα subunits
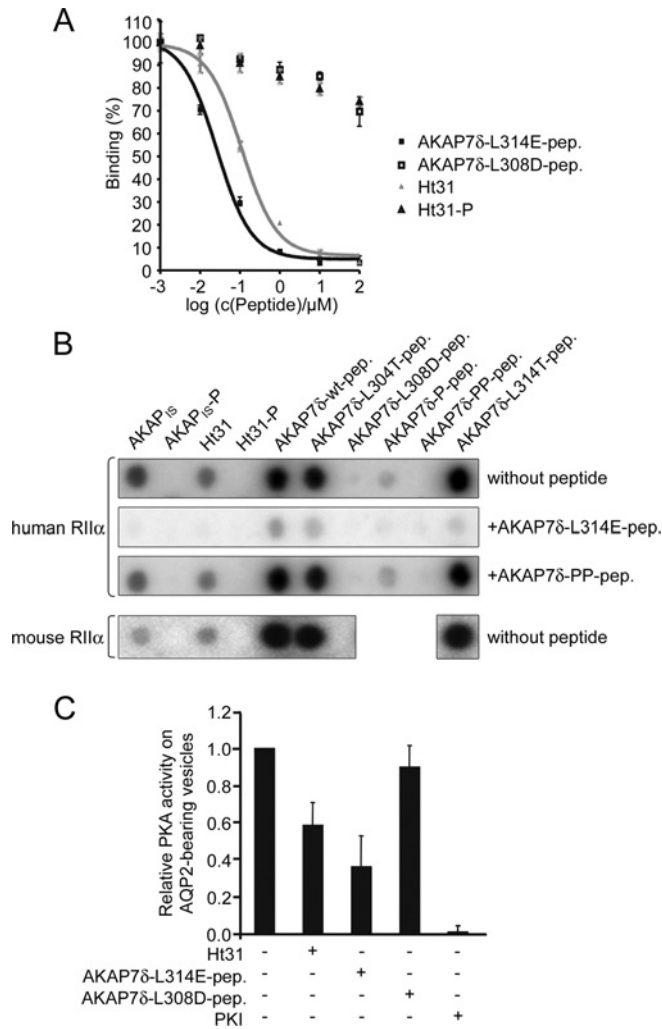
Figure 2 AKAP7δ-derived peptides act as PKA-anchoring disruptors *in vitro*

The sequences of the peptides are given in Table 1. (**A**) Multiwell plates were coated with RIIα subunits (15 ng/well) and incubated with GST–AKAP7δ (15 ng/well) in the presence of the indicated peptides. Binding of GST–AKAP7δ to RIIα subunits was detected by incubation with anti-AKAP7δ and secondary horseradish peroxidase-conjugated antibodies, and subsequently with a chemiluminescence peroxidase substrate solution. Signals were recorded in a luminescence intensity reader ($n = 3$; means $\pm$ S.D.). (**B**) Peptides representing the RII-binding domain of AKAP7δ, derivatives thereof, Ht31 and AKAP$_{IS}$ were SPOT-synthesized and probed with ^{32}P-labelled RIIα subunits alone (upper panel), in the presence of the PKA-anchoring disruptor peptide AKAP7δ-L314E-pep (10 μM; middle panel) or the inactive control peptide AKAP7δ-PP-pep (10 μM; lower panel). Signals were detected by autoradiography. A representative experiment is shown ($n = 3$ independent experiments). (**C**) AQP2-bearing vesicles were isolated from rat renal inner medullary tissue. The vesicles were left untreated or incubated with the peptides Ht31, AKAP7δ-L314E-pep, AKAP7δ-L308D-pep (100 μM each) or the PKA inhibitor peptide PKI (100 μM), and PKA activity was assayed ($n = 3$; means $\pm$ S.D.).

with a proline-containing AKAP7δ-PP-pep control peptide did not affect the interaction.

AKAP7δ-derived peptides disrupt PKA anchoring *in vitro*

The high-affinity binding of AKAP7δ-derived peptides to RIIα subunits suggests that such peptides act as potent disruptors of PKA anchoring. Indeed, in an ELISA-based assay (Figure 2A), peptide AKAP7δ-L314E-pep inhibited the AKAP7δ-RIIα interaction with an IC$_{50}$ of 26 ± 4 nM. This value is approx. 5-fold lower than that obtained for the peptide Ht31 (IC$_{50} = 113 \pm 17$ nM). The proline-containing peptides AKAP7δ-PP-pep and
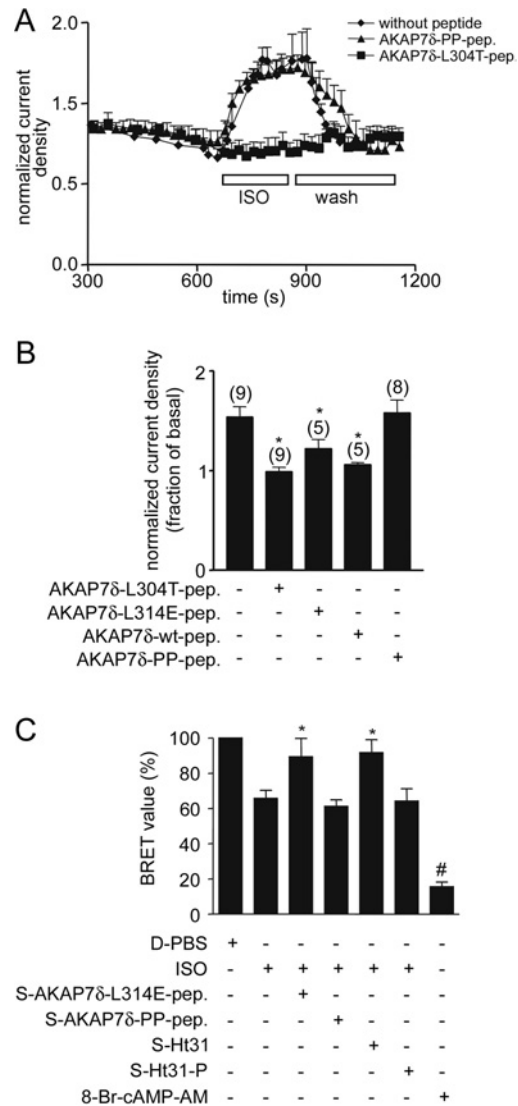
Figure 3 AKAP7δ-derived peptides disrupt AKAP–PKA interactions *in vivo*

The sequences of the peptides are given in Table 1. (**A**) L-type Ca^{2+}-channel currents were measured in rat neonatal cardiac myocytes by using the patch-clamp technique. Cells were clamped to -70 mV and repetitively depolarized to a test potential of 0 mV after a 400 ms ramp to -35 mV. The peptides AKAP7δ-L304T-pep, AKAP7δ-L314E-pep or the inactive control peptide AKAP7δ-PP-pep (30 μM each) and AKAP7δ-wt-pep (1 μM) were administered through the patch pipette. Current recordings started 400 s after establishing whole-cell configuration. Cells were stimulated with isoproterenol (1 μM; ISO) at the indicated time followed by a washout. Time courses of normalized current densities (**A**) and a summary (**B**) of the individual experiments (n is indicated by the numbers in brackets, means $\pm$ S.E.M.). *, significant difference from untreated control ($P < 0.05$). (**C**) COS-7 cells expressing human RIIα subunits fused with GFP, and Cα subunits fused with luciferase were grown in 96-well plates. Cells were treated with the stearate-coupled peptides S–AKAP7δ-L314E-pep, S–AKAP7δ-PP-pep, S–Ht31, S–Ht31-P (100 μM each), 8-Br-cAMP-AM (50 μM) or D-PBS for 30 min. Subsequently, isoproterenol (ISO; 100 μM, 10 min) was added where indicated. BRET was measured by using luciferase substrate DeepBlueC^{TM} and a multilabel reader (two to four experiments per condition with $n = 6$ wells of cells for each measurement; means $\pm$ S.E.M.). BRET values obtained for D-PBS-treated cells expressing the sensor were defined as 100 %. Statistical analysis was carried out using Prism 4.0. Data were analysed by one-way ANOVA using the Newman-Keuls test to identify significant differences compared with cells treated with D-PBS. *, $P < 0.05$; #, $P < 0.001$.

Ht31-P which do not bind RII subunits (see above) did not inhibit the interaction.

Human or mouse RIIα subunits (Figure 2B) or a combination of bovine RIIα and RIIβ subunits (results not shown) bound to
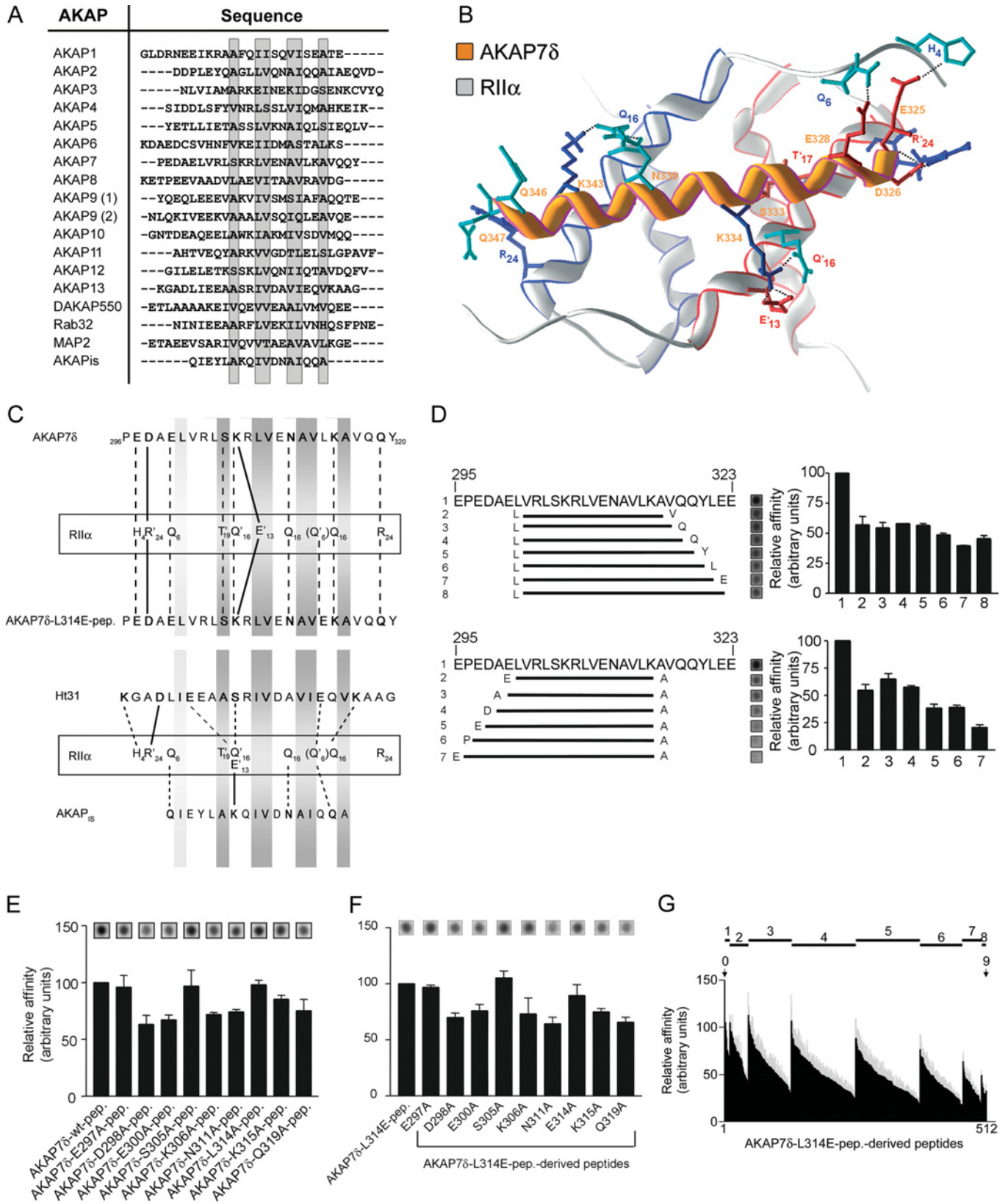
Figure 4   Determinants of the high-affinity interaction of the AKAP7δ RII-binding domains with RIIα subunits

(**A**) Alignment of RII-binding domains of the indicated AKAPs. Conserved amino acid residues are indicated in grey, and the two RII-binding domains of AKAP9 by (1) and (2). (**B**) Structural model showing the interaction (top view) of the RII-binding domain of AKAP7δ (helix, orange, residues 296–320 of AKAP7δ) with the dimer of RIIα subunits (the light grey backbones of the two monomers are verged in red and blue respectively). Essential interacting hydrophilic side-chains of polar (green) or charged (red, negative; blue, positive) amino acid residues are displayed and labelled by a single letter code and the position within the protein. (**C**) Schematic representation of the interaction between RIIα subunits and the RII-binding domain of AKAP7δ (corresponds to peptide

SPOT-synthesized AKAP7δ-derived peptides, Ht31 or AKAP$_{IS}$, indicating that interactions of the peptides with RIIα subunits are not restricted to RIIα subunits from a particular species. Pre-incubation of ^{32}P-labelled RIIα subunits with the peptide AKAP7δ-L314E-pep (10 μM) abolished RIIα-binding to the SPOT-synthesized peptides AKAP$_{IS}$ and Ht31, and strongly decreased its binding to the SPOT-synthesized peptides AKAP7δ-wt-pep, AKAP7δ-L304T-pep and AKAP7δ-L314E-pep (Figure 2B). The control peptide AKAP7δ-PP-pep did not apparently affect the interaction of RIIα subunits with the SPOT-synthesized peptides, indicating that the AKAP7δ-derived peptide AKAP7δ-L314E-pep is suitable as a potent competitive blocker in RII overlay assays.

Peptide-based disruption of PKA anchoring *in vitro* was further tested on AQP2-bearing vesicles, to which PKA is anchored by AKAP7δ [25]. The peptides AKAP7δ-L314E-pep and Ht31 (each 10 μM) were chosen for the analysis in order to compare their potency to disrupt PKA anchoring. Each of the peptides decreased PKA activity by approx. 50 % (Figure 2C). The control peptide AKAP7δ-L308D-pep, which does not bind RII subunits (Table 2) did not affect PKA activity. By contrast, the PKA inhibitor peptide PKI-(5–24) ablated vesicular PKA activity, indicating that PKA is anchored to the vesicles by AKAPs and, in addition, by other means, such as interaction with proteins through non-canonical RII-binding domains.

In vivo disruption of PKA-anchoring using AKAP7δ-derived peptides

The efficiency of the AKAP7δ-derived peptides to disrupt PKA anchoring in a cellular system was evaluated by interference with PKA anchoring in neonatal cardiac myocytes and COS-7 cells. In cardiac myocytes, L-type Ca^{2+} channels are phosphorylated by PKA in response to β-adrenergic receptor activation [37,41,42]. Phosphorylation increases the open-probability of the channels and is a key event in β-adrenergic-receptor-mediated increases in myocyte contractility. Global uncoupling of PKA from AKAPs with the peptide Ht31 prevented β-adrenergic receptor-mediated increases in L-type Ca^{2+} channel currents in adult rat cardiac myocytes [37]. Similarly, an AKAP7α-derived peptide mimicking the domain (leucine zipper motif) of AKAP7α that mediates direct interaction with L-type Ca^{2+} channels had a similar effect [37]. Figures 3(A) and 3(B) depict patch-clamp experiments using rat neonatal cardiac myocytes which show that the peptides AKAP7δ-L304T-pep and AKAP7δ-L314E-pep also prevented isoproterenol (β-adrenergic receptor agonist)-induced PKA-dependent increases in L-type Ca^{2+} channel currents in these cells at a concentration of 30 μM. Peptide AKAP7δ-wt-pep was partially insoluble at a concentration of 30 μM and was therefore used at 1 μM. At this concentration it prevented the isoproterenol-induced increase in L-type channel current to the same extent

as the peptides AKAP7δ-L304T-pep and AKAP7δ-L314E-pep. The control peptide AKAP7δ-PP-pep, which does not bind RIIα subunits (as described above), did not alter L-type Ca^{2+} channel currents at either 1 or 30 μM concentration (Figures 3A and 3B).

Stearate-coupled or myristoylated versions of the peptide, Ht31, disrupt PKA anchoring in cells [31]. We coupled AKAP7δ-derived peptides AKAP7δ-L314E-pep and AKAP7-PP-pep to stearate (S–AKAP7δ-L314E-pep and S–AKAP7δ-PP-pep respectively) and compared their cellular effects with those of stearate-coupled Ht31 (S–Ht31), and proline-containing Ht31-P (S–Ht31-P; Figure 3C). A recently characterized BRET-based sensor consisting of human RIIα subunits fused with luciferase and human Cα subunits fused with GFP was used to detect PKA anchoring [38]. The sensor forms a PKA holoenzyme and dissociates in response to the elevation of cAMP, which is reflected by a decrease in the BRET signal. The sensor was expressed in COS-7 cells endogenously expressing β-adrenergic receptors to which PKA is anchored via AKAP5 [43,44]. Elevation of cAMP levels by β-adrenergic receptor stimulation with isoproterenol or by incubaton of the cells with the membrane-permeable cAMP analogue 8-Br-cAMP-AM (50 μM), caused a decrease of the BRET signal by 35–40 % and 90 % respectively. Thus as expected a uniform rise in cAMP elicits higher overall PKA activation than a local rise of cAMP induced by receptor stimulation. When the cells were pre-incubated with the peptides S–AKAP7δ-L314E-pep or S–Ht31 prior to isoproterenol treatment, the probe was displaced from the plasma membrane (results not shown) and the BRET signal was only decreased by approx. 10 %, indicating that the peptides entered the cells, prevented dissociation of the sensor and thus largely ablated local activation of PKA (Figure 3C). However, the level of peptide uptake and the kinetics of the uptake into the cells are not known at present. Control peptides S–AKAP7δ-PP-pep or S–Ht-31-PP had no effect on the cellular distribution of the sensor (results not shown) and did not change the BRET signal upon isoproterenol treatment. Taken together, the results show that the AKAP7δ-derived peptides act as potent PKA-anchoring disruptors *in vitro* and *in vivo*.

Hydrophobic, polar and charged amino acid residues contribute to AKAP–PKA interactions

Next we set out to define the molecular basis of the high-affinity interaction between the RII-binding domain of AKAP7δ and RII subunits. An alignment of the RII-binding domains of 18 known AKAPs (Figure 4A) indicated the presence of polar and hydrophobic (shaded in grey) amino acid residues in conserved positions. A peptide substitution array of the AKAP7δ RII-binding domain (results not shown) also documented the relevance

AKAP7δ-wt-pep) and the peptides AKAP7δ-L314E-pep (top panel), AKAP$_{IS}$ and Ht31 (lower panel). Amino acid residues that potentially form hydrogen bonds or salt-bridges are connected by dotted and unbroken lines respectively. Hydrophobic amino acid residues are highlighted in grey. The residues of the two RIIα protomers are distinguishable by the absence and presence of apostrophes. (**D**) The peptides comprising the RII-binding domain of AKAP7δ (amino acid residues 295–323) and the indicated N- and C-terminally truncated mutants (black lines) were SPOT-synthesized and probed with ^{32}P-labelled RIIα subunits. Interaction was detected by autoradiography. Representative spots from three independent experiments are shown. The signals were quantified by densitometric analysis. The relative affinity of each peptide for RIIα binding is depicted as the ratio of its signal intensity to that of the peptide AKAP7δ-wt-pep (mean ± S.D.). The numbers in the left and right panels denote the same peptides. (**E**)–(**G**) Putative hydrogen bond- and salt-bridge-forming amino acid residues of AKAP7δ-derived peptides contribute to RII-binding. Peptide substitution arrays were generated where each potential hydrogen bond- or salt-bridge-forming amino acid residue (see Figure 4C) of the peptides AKAP7δ-wt-pep (**E**) and AKAP7δ-L314E-pep (**F**) were substituted with alanine. The peptides were probed for binding to ^{32}P-labelled RII subunits. Representative data from three independent experiments are shown. Signals were visualized by autoradiography and quantified densitometrically (means ± S.D.). (**G**) The peptides AKAP7δ-wt-pep, AKAP7δ-L314E-pep, and derivatives of the peptide AKAP7δ-L314E-pep in which all potential hydrogen-bond- or salt-bridge-forming amino acid residues were replaced by alanine in all possible combinations (512 peptides) were SPOT-synthesized. The sequences of the peptides are given in Supplementary Table 1 (http://www.BiochemJ.org/bj/396/bj3960297add.htm). The peptides were subjected to RII overlay assays. Signals were visualized by autoradiography and quantified densitometrically. The relative binding affinities of each peptide, normalized to that of the peptide AKAP7δ-wt-pep (means ± S.D.) are shown. The numbers at top of the graph indicate the numbers of amino acid residue substitutions. The black lines mark blocks of peptides containing the same number but different combinations of substitutions. Within each block the peptides are ordered according to their relative affinity.

of hydrophobic amino acid residues in conserved positions and in addition the efficiency of proline to lower or disrupt RII binding (see Figure 1A and Table 2). Molecular modelling of the interaction between the RII-binding domain of AKAP7δ (amino acid residues 296–320) and RIIα subunits (amino acid residues 1–44; Figure 4B) again revealed hydrophobic contacts. The amino acid residues involved correspond to those suggested by the alignment depicted in Figure 4(A). In addition, the model suggested that polar and charged amino acid residues within the RII-binding domain contribute to the interaction. A total of seven out of 13 such amino acid residues may form hydrogen bonds (Glu[297], Glu[300], Ser[305], Lys[306], Asn[311], Lys[315] and Gln[319]) with partners in the RIIα subunit dimer. One amino acid residue (Asp[298]) may form a salt-bridge with Arg[24] of RIIα and one (Lys[306]) may form either a hydrogen bond with Gln[16] or a salt-bridge with Glu[13] of RIIα. This is depicted schematically in Figure 4(C), which also indicates potential hydrogen bonds and salt-bridges between the peptides AKAP7δ, AKAP7δ-L314E-pep, Ht31 and AKAP$_{IS}$, and RIIα subunits.

In order to test whether non-hydrophobic contacts play a role in the interaction between AKAP7δ and RIIα subunits, a peptide encompassing the RII-binding domain of AKAP7δ (amino acid residues 295–323), and a series of truncation mutants of this peptide, were SPOT-synthesized and probed with ^{32}P-labelled RIIα subunits (Figure 4D). N-terminal truncation of 1–5 amino acid residues removed three predicted interacting residues (Glu[297], Asp[298] and Glu[300]) from the RII-binding domain. C-terminal truncation of 1–6 amino acid residues removed one residue (Gln[319]) predicted to be involved in the interaction. Indeed, removing the relevant amino acid residues at either the N- or C-terminus resulted in decreased RII binding. Next, the influences of single amino acid residues in the RII-binding domain of AKAP7δ that potentially form hydrogen bonds or salt-bridges with residues of RIIα subunits were tested by utilizing a combination of peptide SPOT-synthesis and RII overlay. For this purpose, the peptide AKAP7δ-wt-pep and mutants with alanine substitutions at the relevant positions indicated in Figure 4(C) were SPOT-synthesized and probed with ^{32}P-labelled RIIα subunits. Figure 4(E) shows that the substitutions did not apparently affect the interaction, or resulted in decreased binding of the peptides to RIIα subunits. The replacement of the charged amino acid residues Asp[298] and Glu[300] by alanine decreased binding to a similar extent as an N-terminal truncation, removing these residues from peptide 5 as shown in the upper panel of Figure 4(D). Similarly, both substitution of the polar Gln[319] with alanine or its removal by truncation as in peptide 6, shown in the lower panel of Figure 4(D), decreased the binding to RII subunits.

The K_d values for the interaction of the peptides AKAP7δ-wt-pep and AKAP7δ-L314E-pep with RIIα subunits were similar (Figure 1, Table 2). However, peptide AKAP7δ-wt-pep partially precipitated at a concentration of 30 μM limiting its experimental application (as described above). Peptide AKAP7δ-L314E-pep was still soluble at concentrations above 100 μM, indicating that the introduction of a glutamic acid residue increases its solubility. Owing to its higher solubility, AKAP7δ-L314E-pep is the most widely applicable peptide with which to study PKA anchoring. Its interaction with RII subunits was further analysed. As in the AKAP7δ-wt-pep peptide, replacement of hydrogen-bond- or salt-bridge-forming amino acid residues with alanine did not influence the interaction with RIIα subunits, or decreased it (Figure 4F). Moreover, particular combinations of two or more amino acid residue substitutions in the peptide AKAP7δ-L314E-pep (2^9 possibilities) did not apparently affect the interaction of the peptides with RII subunits, or decreased it but did not abolish the interaction (Figure 4G; and Supplementary Table 1).

Taken together, the results indicate that hydrophobic amino acid residues in the amphipathic helix form the backbone for the interaction of the AKAP7δ RII-binding domain with RII subunits and, in addition, that the binding is increased by charged and polar amino acid residues on the hydrophilic face of the helix, presumably through intermolecular hydrogen bond or salt-bridge formation.

DISCUSSION

Various cellular processes depend upon the interaction of PKA with AKAPs (for review see [2–4]). For example, AKAP–PKA interactions are a prerequisite for vasopressin-induced AQP2 redistribution and thus water reabsorption in renal principal cells [25,31]. In cardiac myocytes, the tethering of PKA by AKAPs allows for β-adrenergic receptor-mediated increases in L-type Ca^{2+} channel currents and thereby for increased contractility [37]. We have identified novel high affinity AKAP7δ-derived peptides, which effectively inhibit PKA–AKAP interactions under various experimental conditions *in vitro* and in cells. For example, they prevent β-adrenergic receptor-mediated increases in L-type Ca^{2+} channel currents in patch-clamp experiments (Figures 3A and 3B). Stearate-coupled membrane-permeable versions of the AKAP7δ-derived peptides decrease β-adrenergic receptor-mediated activation of PKA (Figure 3), presumably by displacing PKA from locations that are in close proximity to the receptor and adenylate cyclase. Thus the AKAP7δ-derived peptides represent effective tools with which to study PKA anchoring.

The observation that disruption of PKA–AKAP interactions in cardiac myocytes prevents β-adrenergic receptor-mediated increases in L-type Ca^{2+} channel currents is reminiscent of the effect of β-blockers on cardiac myocytes. β-blockers dampen the effects of adrenergic stimuli on the heart, and are applied for the treatment of cardiovascular disease. Thus it appears that PKA–AKAP interaction sites are suitable drug targets. A detailed insight into the molecular mechanisms underlying AKAP–PKA interactions may provide the basis for the design of non-peptidic small molecules disrupting AKAP–PKA interactions. The targeting of intracellular protein–protein interactions involving scaffolding proteins such as AKAPs significantly widens the basis for drug therapy by introducing a novel class of drugs that acts independently of ion channels, receptors and enzymes (as classical drugs do).

In order to gain further insight into the interaction of PKA and AKAPs, we aimed to elucidate the determinants defining the high-affinity interaction of the RII-binding domain of AKAP7δ with RIIα subunits. Previous studies have shown that the interaction between RII subunits and RII-binding domains involve hydrophobic amino acid residues of the amphipathic helix forming the RII-binding domain [16,21]. Our studies confirm this observation for AKAP7δ. Furthermore, they indicate that additional factors safeguard the interaction and influence the binding affinity. Peptides comprising 25 amino acid residues derived from the RII-binding domain of AKAP7δ bind RIIα subunits with a sub-nanomolar K_d; truncation mutants bind RIIα subunits less efficiently (Figure 4D). This observation cannot be explained by the loss of hydrophobic contacts. It is likely that polar or charged amino acid residues contribute directly to the interaction. According to the structural model (Figure 4B), seven out of 13 polar or charged amino acid residues in the AKAP7δ RII-binding domain can form hydrogen bonds with partners in the binding pocket of the RIIα dimer (Figures 4B and 4C). Indeed, substitution of alanine for several of the potential hydrogen-forming amino acid residues decreased the binding affinity to RIIα subunits

(Figures 4E–4G). The argument is further supported by the finding that AKAP7δ-derived peptides of the same length substituted with oppositely charged amino acid residues bind RIIα subunits significantly less than wt peptides (e.g. D298R and E300R; results not shown). The substitution of alanine in position 311 for asparagine (N311A) led to a strong decrease in RIIα subunit binding (Figure 4E). This asparagine is conserved in the high-affinity AKAPs, AKAP7δ, AKAP2, AKAP5, AKAP12, and in AKAP$_{IS}$ (Figure 4A). None of the tested alanine-substituted peptides lost the ability to bind to RIIα subunits (Figure 4E), suggesting that the interaction is mediated by hydrophobic amino acid residues retained in the peptides. Thus intermolecular hydrogen bonds (and salt-bridges) between the amphipathic helix-forming RII-binding domain of AKAPs and RIIα subunits are likely to contribute to the high-affinity binding.

REFERENCES

1 Zaccolo, M. and Pozzan, T. (2002) Discrete microdomains with high concentration of cAMP in stimulated rat neonatal cardiac myocytes. Science (Washington) **295**, 1711–1715

2 Langeberg, L. K. and Scott, J. D. (2005) A-kinase-anchoring proteins. J. Cell Sci. **118**, 3217–3220

3 Tasken, K. and Aandahl, E. M. (2004) Localized effects of cAMP mediated by distinct routes of protein kinase A. Physiol. Rev. **84**, 137–167

4 Wong, W. and Scott, J. D. (2004) AKAP signalling complexes: focal points in space and time. Nat. Rev. Mol. Cell Biol. **5**, 959–970

5 Mongillo, M., McSorley, T., Evellin, S., Sood, A., Lissandron, V., Terrin, A., Huston, E., Hannawacker, A., Lohse, M. J., Pozzan, T. et al. (2004) Fluorescence resonance energy transfer-based analysis of cAMP dynamics in live neonatal rat cardiac myocytes reveals distinct functions of compartmentalized phosphodiesterases. Circ. Res. **95**, 67–75

6 Baillie, G. S., Scott, J. D. and Houslay, M. D. (2005) Compartmentalisation of phosphodiesterases and protein kinase A: opposites attract. FEBS Lett. **579**, 3264–3270

7 Jin, J., Smith, F. D., Stark, C., Wells, C. D., Fawcett, J. P., Kulkarni, S., Metalnikov, P., O'Donnell, P., Taylor, P., Taylor, L. et al. (2004) Proteomic, functional, and domain-based analysis of in vivo 14-3-3 binding proteins involved in cytoskeletal regulation and cellular organization. Curr. Biol. **14**, 1436–1450

8 Baisamy, L., Jurisch, N. and Diviani, D. (2005) Leucine zipper-mediated homo-oligomerization regulates the Rho-GEF activity of AKAP-Lbc. J. Biol. Chem. **280**, 15405–15412

9 Carnegie, G. K., Smith, F. D., McConnachie, G., Langeberg, L. K. and Scott, J. D. (2004) AKAP-Lbc nucleates a protein kinase D activation scaffold. Mol. Cell **15**, 889–899

10 Diviani, D., Soderling, J. and Scott, J. D. (2001) AKAP-Lbc anchors protein kinase A and nucleates Gα 12-selective Rho-mediated stress fiber formation. J. Biol. Chem. **276**, 44247–44257

11 Diviani, D., Abuin, L., Cotecchia, S. and Pansier, L. (2004) Anchoring of both PKA and 14-3-3 inhibits the Rho-GEF activity of the AKAP-Lbc signaling complex. EMBO J. **23**, 2811–2820

12 Klussmann, E., Edemir, B., Pepperle, B., Tamma, G., Henn, V., Klauschenz, E., Hundsrucker, C., Maric, K. and Rosenthal, W. (2001) Ht31: the first protein kinase A anchoring protein to integrate protein kinase A and Rho signaling. FEBS Lett. **507**, 264–268

13 Herberg, F. W., Taylor, S. S. and Dostmann, W. R. (1996) Active site mutations define the pathway for the cooperative activation of cAMP-dependent protein kinase. Biochemistry **35**, 2934–2942

14 Kim, C., Xuong, N. H. and Taylor, S. S. (2005) Crystal structure of a complex between the catalytic and regulatory (RIα) subunits of PKA. Science (Washington) **307**, 690–696

15 Colledge, M. and Scott, J. D. (1999) AKAPs: from structure to function. Trends Cell Biol. **9**, 216–221

16 Banky, P., Roy, M., Newlon, M. G., Morikis, D., Haste, N. M., Taylor, S. S. and Jennings, P. A. (2003) Related protein-protein interaction modules present drastically different surface topographies despite a conserved helical platform. J. Mol. Biol. **330**, 1117–1129

17 Carr, D. W., Stofko-Hahn, R. E., Fraser, I. D., Bishop, S. M., Acott, T. S., Brennan, R. G. and Scott, J. D. (1991) Interaction of the regulatory subunit (RII) of cAMP-dependent protein kinase with RII-anchoring proteins occurs through an amphipathic helix binding motif. J. Biol. Chem. **266**, 14188–14192

18 Newlon, M. G., Roy, M., Morikis, D., Carr, D. W., Westphal, R., Scott, J. D. and Jennings, P. A. (2001) A novel mechanism of PKA anchoring revealed by solution structures of anchoring complexes. EMBO J. **20**, 1651–1662

19 Vijayaraghavan, S., Liberty, G. A., Mohan, J., Winfrey, V. P., Olson, G. E. and Carr, D. W. (1999) Isolation and molecular characterization of AKAP110, a novel, sperm-specific protein kinase A-anchoring protein. Mol. Endocrinol. **13**, 705–717

20 Dransfield, D. T., Bradford, A. J., Smith, J., Martin, M., Roy, C., Mangeat, P. H. and Goldenring, J. R. (1997) Ezrin is a cyclic AMP-dependent protein kinase anchoring protein. EMBO J. **16**, 35–43

21 Alto, N. M., Soderling, S. H., Hoshi, N., Langeberg, L. K., Fayos, R., Jennings, P. A. and Scott, J. D. (2003) Bioinformatic design of A-kinase anchoring protein-in silico: a potent and selective peptide antagonist of type II protein kinase A anchoring. Proc. Natl. Acad. Sci. U.S.A. **100**, 4445–4450

22 Carr, D. W., Hausken, Z. E., Fraser, I. D., Stofko-Hahn, R. E. and Scott, J. D. (1992) Association of the type II cAMP-dependent protein kinase with a human thyroid RII-anchoring protein. Cloning and characterization of the RII-binding domain. J. Biol. Chem. **267**, 13376–13382

23 Herberg, F. W., Maleszka, A., Eide, T., Vossebein, L. and Tasken, K. (2000) Analysis of A-kinase anchoring protein (AKAP) interaction with protein kinase A (PKA) regulatory subunits: PKA isoform specificity in AKAP binding. J. Mol. Biol. **298**, 329–339

24 Klussmann, E. and Rosenthal, W. (2006) AKAP7. AfCS-Nature Molecule Pages, doi: 10.1038/mp.A000246

25 Henn, V., Edemir, B., Stefan, E., Wiesner, B., Lorenz, D., Theilig, F., Schmitt, R., Vossebein, L., Tamma, G., Beyermann, M. et al. (2004) Identification of a novel A-kinase anchoring protein 18 isoform and evidence for its role in the vasopressin-induced aquaporin-2 shuttle in renal principal cells. J. Biol. Chem. **279**, 26654–26665

26 Newlon, M. G., Roy, M., Morikis, D., Hausken, Z. E., Coghlan, V., Scott, J. D. and Jennings, P. A. (1999) The molecular basis for protein kinase A anchoring revealed by solution NMR. Nat. Struct. Biol. **6**, 222–227

27 Oksche, A., Boese, G., Horstmeyer, A., Furkert, J., Beyermann, M., Bienert, M. and Rosenthal, W. (2000) Late endosomal/lysosomal targeting and lack of recycling of the ligand-occupied endothelin B receptor. Mol. Pharmacol. **57**, 1104–1113

28 Frank, R. (2002) The SPOT-synthesis technique. Synthetic peptide arrays on membrane supports–principles and applications. J. Immunol. Methods **267**, 13–26

29 Kramer, A. and Schneider-Mergener, J. (1998) Synthesis and screening of peptide libraries on continuous cellulose membrane supports. Methods Mol. Biol. **87**, 25–39

30 Bregman, D. B., Bhattacharyya, N. and Rubin, C. S. (1989) High affinity binding protein for the regulatory subunit of cAMP-dependent protein kinase II-B. Cloning, characterization, and expression of cDNAs for rat brain P150. J. Biol. Chem. **264**, 4648–4656

31 Klussmann, E., Maric, K., Wiesner, B., Beyermann, M. and Rosenthal, W. (1999) Protein kinase A anchoring proteins are required for vasopressin-mediated translocation of aquaporin-2 into cell membranes of renal principal cells. J. Biol. Chem. **274**, 4934–4938

32 Chen, Y. H., Yang, J. T. and Martinez, H. M. (1972) Determination of the secondary structures of proteins by circular dichroism and optical rotatory dispersion. Biochemistry **11**, 4120–4131

33 Case, D. A., Pearlman, D. A., Caldwell, J. W., Cheatham, III, T. E., Wang, J., Roos, W. S., Simmerling, C. L., Darden, T. A., Merz, K. M., Stanton, R. V. et al. (2002) AMBER 7 program. 2002. University of California, San Francisco, U.S.A.

34 Laskowski, R. A., Rullmann, J. A., MacArthur, M. W., Kaptein, R. and Thornton, J. M. (1996) AQUA and PROCHECK-NMR: programs for checking the quality of protein structures solved by NMR. J. Biomol. NMR **8**, 477–486

35 Dostal, D. E., Rothblum, K. N., Conrad, K. M., Cooper, G. R. and Baker, K. M. (1992) Detection of angiotensin I and II in cultured rat cardiac myocytes and fibroblasts. Am. J. Physiol. **263**, C851–C863

36 Wang, M., Tashiro, M. and Berlin, J. R. (2004) Regulation of L-type calcium current by intracellular magnesium in rat cardiac myocytes. J. Physiol. **555**, 383–396

37 Hulme, J. T., Lin, T. W., Westenbroek, R. E., Scheuer, T. and Catterall, W. A. (2003) β-adrenergic regulation requires direct anchoring of PKA to cardiac CaV1.2 channels via a leucine zipper interaction with A kinase-anchoring protein 15. Proc. Natl. Acad. Sci. U.S.A. **100**, 13093–13098

38 Prinz, A., Diskar, M., Erlbruch, A. and Herberg, F. W. (2006) Novel, isotype-specific sensors for protein kinase A subunit interaction based on bioluminescence resonance energy transfer (BRET). J. Cell Sci. **119**, in the press

39 Schultz, C., Vajanaphanich, M., Harootunian, A. T., Sammak, P. J., Barrett, K. E. and Tsien, R. Y. (1993) Acetoxymethyl esters of phosphates, enhancement of the permeability and potency of cAMP. J. Biol. Chem. **268**, 6316–6322

40 Lehrman, S. R., Tuls, J. L. and Lund, M. (1990) Peptide α-helicity in aqueous trifluoroethanol: correlations with predicted α-helicity and the secondary structure of the corresponding regions of bovine growth hormone. Biochemistry **29**, 5590–5596

41 Hulme, J. T., Ahn, M., Hauschka, S. D., Scheuer, T. and Catterall, W. A. (2002) A novel leucine zipper targets AKAP15 and cyclic AMP-dependent protein kinase to the C terminus of the skeletal muscle Ca^{2+} channel and modulates its function. J. Biol. Chem. **277**, 4079–4087

42 Hulme, J. T., Scheuer, T. and Catterall, W. A. (2004) Regulation of cardiac ion channels by signaling complexes: role of modified leucine zipper motifs. J. Mol. Cell Cardiol. **37**, 625–631

43 Malbon, C. C., Tao, J. and Wang, H. Y. (2004) AKAPs (A-kinase anchoring proteins) and molecules that compose their G-protein-coupled receptor signalling complexes. Biochem. J. **379**, 1–9

44 Lynch, M. J., Baillie, G. S., Mohamed, A., Li, X., Maisonneuve, C., Klussmann, E., van Heeke, G. and Houslay, M. D. (2005) RNA silencing identifies PDE4D5 as the functionally relevant cAMP phosphodiesterase interacting with β arrestin to control the protein kinase A/AKAP79-mediated switching of the β_2-adrenergic receptor to activation of ERK in HEK293B2 cells. J. Biol. Chem. **280**, 33178–33189